Time Series Analysis of Lake Erie Phytoplankton Dynamics

Final report for the Ohio Lake Erie Commission, Grant number SG-531-2018

3 June 2019

Daniel R. O'Donnell[1], Andrea Conine[1], & James M. Hood[1]

[1]Aquatic Ecology Laboratory, Department of Evolution, Ecology, and Organismal Biology, The Ohio State University

This project was funded through the Lake Erie Protection Fund. The LEPF is supported by tax-deductible donation and voluntary contributions of Ohioans who purchase a Lake Erie license plate featuring the Marblehead lighthouse, Toledo Harbor lighthouse, or the Lake Erie life preserver. For more information, see www.lakeerie.ohio.gov.

Abstract

Global climate change and excessive nutrient loading are rapidly altering the species composition and functioning of aquatic ecosystems. Lake Erie has exemplified this global trend. Changing land use practices and altered precipitation regimes have led to increased bioavailable phosphorus (TBP) loading to the western basin of Lake Erie (WBLE), altering phytoplankton (algae and cyanobacteria) community composition and producing large harmful algal blooms. At an annual scale, it is clear that spring (March – July) TBP loading from the Maumee River is the primary determinate of cyanobacteria bloom extent in WBLE; yet, there has been no comprehensive examination of how nutrient loading and climate have influenced the seasonal dynamics of cyanobacteria or the rest of the phytoplankton community. This is an important knowledge gap because these human induced drivers of environmental change are predicted to have synergistic effects on cyanobacteria bloom timing and extent. Furthermore, we have a poor understanding of what controls the dynamics of the edible phytoplankton taxa that likely support the zooplankton and fish production. Here we combine abiotic and biotic data from the 20-year (1995-2015) Lake Erie Plankton Abundance Survey (LEPAS) with Maumee River nitrogen (N), phosphorus (P), and silica (Si) loading rates and ratios to determine how and why phytoplankton communities have changes in the WBLE. We conducted two sets of analyses. First, we examined seasonal and inter-annual patterns in phytoplankton community dynamics and their mechanistic drivers at one site near the Maumee River mouth. Then, we examined the spatial patterns of phytoplankton community dynamics. This second analysis is ongoing and is not discussed in depth. Supporting previous research, modeling for the first project shows that cyanobacteria blooms increased after 2003 likely due to warmer water temperature as well as recent (preceeding 14-days) and spring TBP loading. The biomass of green algae, diatoms, and cryptophytes also increased between 1995 and 2015. Diatom biomass increased with high rates of NO_3 loading and warm temperatures, whereas green algae and some cryptophytes were favored by cooler water temperatures and high rates of TBP loading. We also observed a considerable advance (> 30 days) in the phenology of both cyanobacteria and diatoms between 1995 and 2015, with an earlier onset and later end to the period of cyanobacteria dominance. Our results highlight that climate warming in conjunction with unchecked nutrient loading will further increase both the size and duration of cyanobacteria blooms and may lead to a decline in cryptophytes which could limit the quantity of edible algae available to zooplankton and higher trophic levels.

Table of Contents

Abstract ***1***

Technical Report ***3***

Project overview **3**

Goals, objectives, and deliverables 3

Changes and hurdles 4

Background **7**

Methods **9**

Datasets 9

Statistical analyses 11

Results **15**

Maumee site manuscript 15

Spatial Patterns manuscript 28

Discussion **29**

Acknowledgements **32**

References **33**

Activities and Timeline ***39***

Deliverables ***40***

Peer-reviewed publications 40

Scientific conference presentations. 40

Postdoc training. 40

Budget ***42***

Technical Report

Project overview

Goals, objectives, and deliverables

The primary goal of our research is to quantify the effects of water temperature and nutrient loading, two key drivers of anthropogenic change, on phytoplankton community succession in the Western Basin of Lake Erie (WBLE) and to determine whether those relationships have changed over the last two decades (i.e., regime shifts). To address this goal, we are analyzing a 20-year phytoplankton community time series from the WBLE (Fig. 1) and focusing on three objectives:

(1) identify patterns in phytoplankton successional dynamics linking spring loading with late-summer cyanobacterial blooms;

(2) determine how phytoplankton succession is mediated by water temperatures and nutrient loading from the Maumee River (both in terms of magnitude and stoichiometry); and

(3) determine whether there have been regime shifts in the linkages between phytoplankton dynamics and nutrient loading.

The combined dataset we utilized (i.e., lake physiochemical data, plankton, and nutrient loading from Maumee River) is characterized by a high degree of complexity and variability in the spatial and temporal dynamics of phytoplankton communities and their putative drivers (nutrient loading, temperature, herbivory, etc.). Therefore, we subdivided this project into two components manuscripts (Fig. 2):

- *Maumee Site manuscript:* examines seasonal and inter-annual patterns in phytoplankton community dynamics and their mechanistic drivers (e.g., nutrient loading, water temperature, and biotic interactions) at one site near the Maumee River mouth (Fig. 1);
- *Spatial Patterns manuscript:* focuses on spatial patterns of phytoplankton community dynamics, differences between low and high nutrient loading years, and the mechanistic drivers of these dynamics at all eight LEPAS sites in the western basin of Lake Erie.

Both manuscripts will address all three objectives. The Maumee Site manuscript has been drafted and will likely be submitted to a peer-reviewed journal in the early Fall. Analysis for Spatial Analysis manuscript is currently in ongoing.

Changes and hurdles

The major complication we confronted was associated with recruiting and retaining a postdoctoral associate for whom the majority of the budget was allocated. Dr. Andrea Conine, the first postdoctoral associate, worked on the project for approximately six months (7 May 2018 to 16 November 2018). Before leaving, she generated a first draft of the Maumee Site manuscript and completed the first round of analyses for the Spatial Patterns manuscript. At that point, she resigned to take a permanent position at the New York Department of Environmental Conservation. Two subsequent searches for a replacement postdoctoral associate failed. We are returning the remainder of those funds. Dr. Danny O'Donnell joined Dr. Hood's lab group on 4 April 2019 and agreed to take on these two manuscripts in addition to work associated with the grant which funds his position.

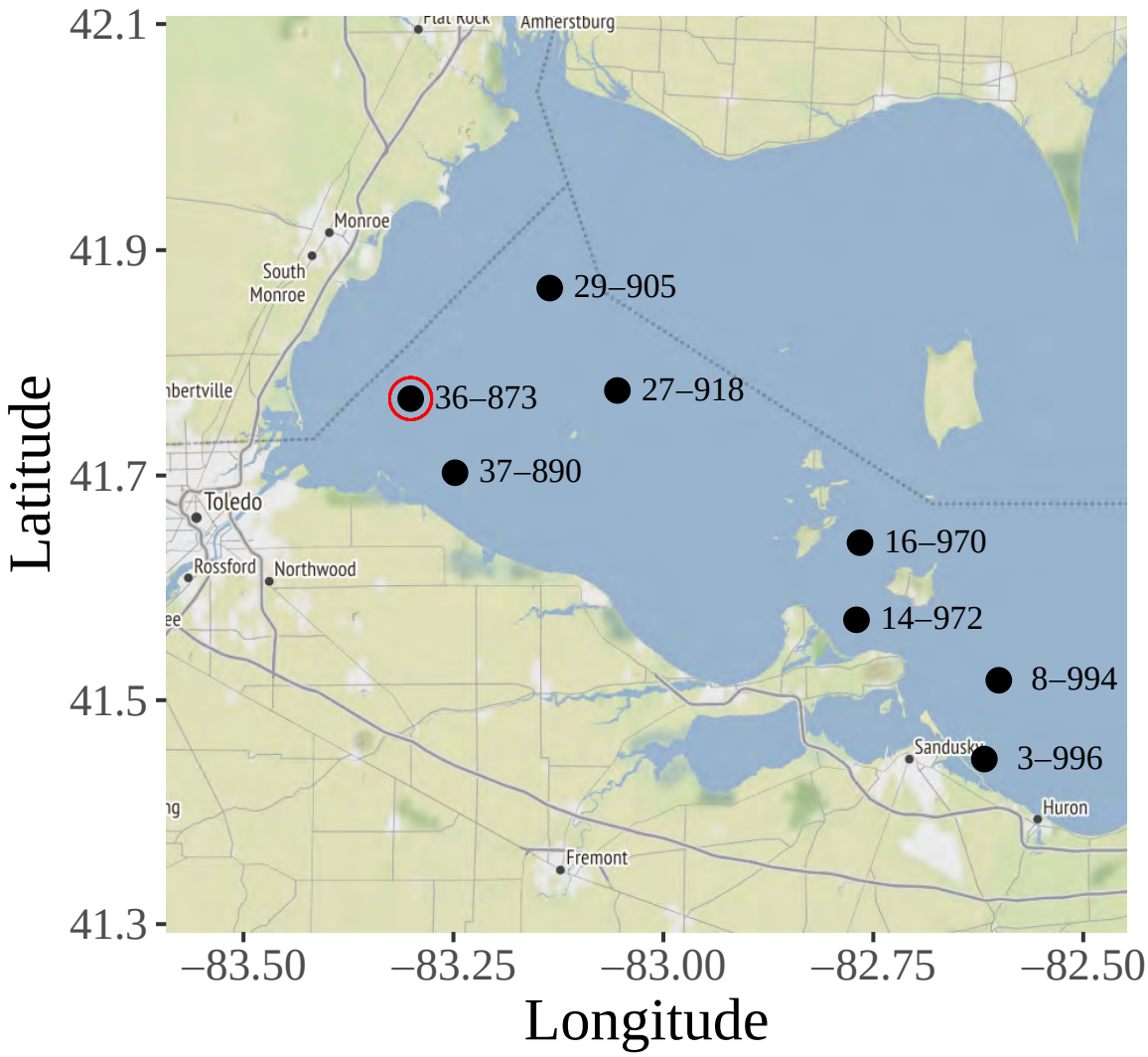

Figure 1. The Western Basin of Lake Erie. Black points are LEPAS sampling locations, labeled with their respective site identification numbers. The point circled in red is the Maumee River mouth sampling location (36-873), which is the focus of our first manuscript.

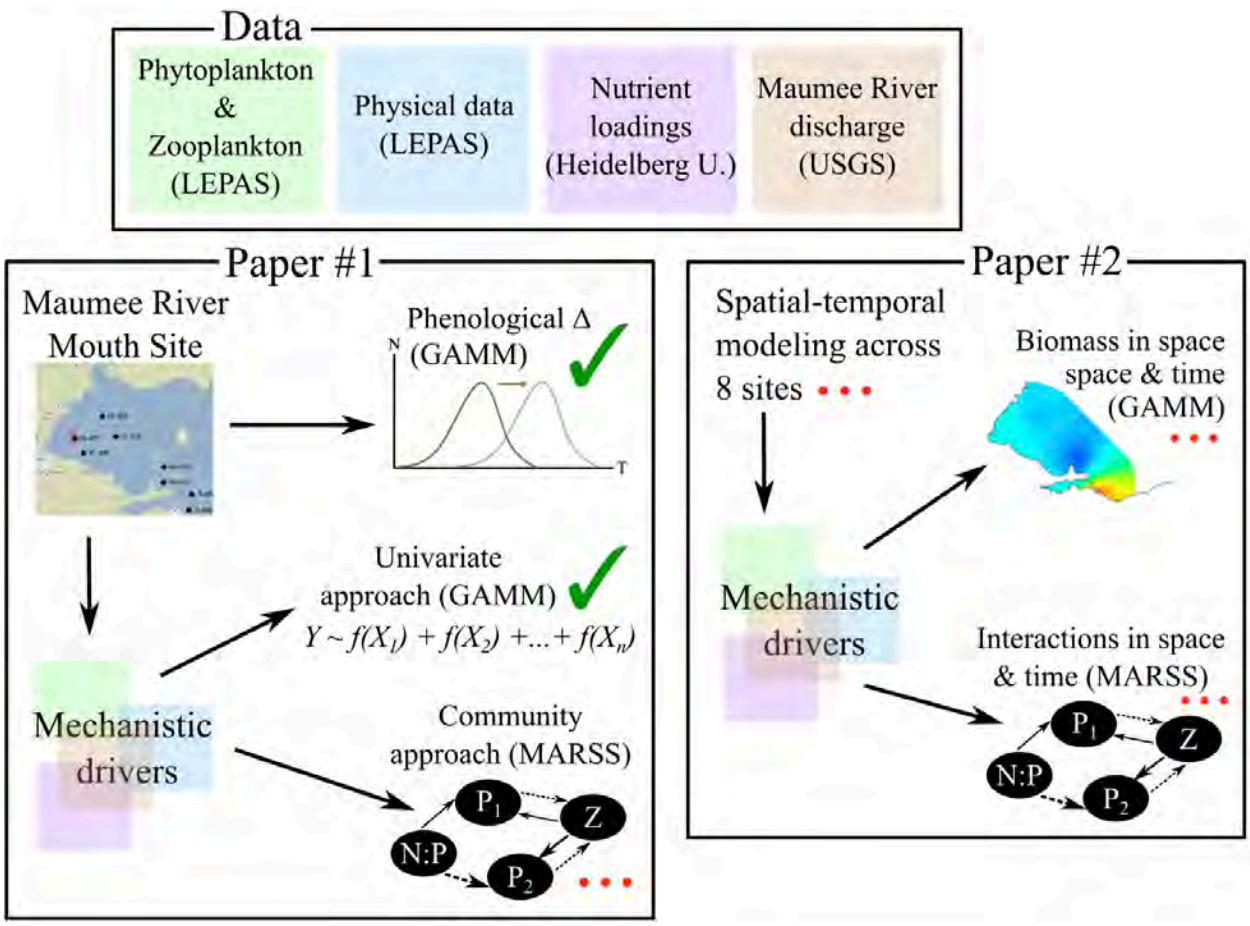

Figure 2. Diagram explaining the workflow for projects undertaken as part of this grant. A green check mark indicates modeling that is complete or nearly complete. Three red dots indicate modeling that is in progress.

Background

The combined effects of climate change and nutrient loading have dramatically altered the structure of the Lake Erie phytoplankton community over the past two decades (Michalak et al. 2013, Scavia et al. 2014, Stumpf et al. 2016). Extreme weather events are occurring with increasing frequency and intensity, causing runoff of agricultural nutrients into rivers and thence into the lake, where excessive loading of nitrogen (N) and phosphorus (P) can trigger harmful algal blooms (HABs; Michalak et al. 2013, Brooks et al. 2016, Stumpf et al. 2016). While this phenomenon has been extensively studied, it is unclear how the timing, magnitude and stoichiometry (elemental ratios of carbon [C], N, P and silica [Si]) of episodic river discharge interact with other climatic variables (e.g. water temperature) to structure Lake Erie phytoplankton community dynamics at both intra- and interannual timescales. Predicting response of phytoplankton communities to environmental change requires a nuanced understanding both of the direct effects of nutrient enrichment and climate on population dynamics (Stumpf et al. 2012, Stumpf et al. 2016) and of indirect effects manifested through biotic interactions (e.g., competition or herbivory; Hampton et al. 2006, Carey et al. 2017).

While interannual patterns in spring P loading is a strong predictor of maximum cyanobacteria bloom extent, the timing of nutrient pulses, warm air temperatures, and low-wind periods are also important determinates of phytoplankton dynamics. For instance, Michalak et al. (2013) hypothesized that the record-setting 2011 bloom of the toxic cyanobacterium *Microcystis* sp. in Lake Erie resulted from a particular sequence of events: 1) unusually high spring precipitation events leading to record-setting bioavailable P loading into Lake Erie; 2) higher than average summer water temperatures (~3°C higher than the 1991-2011 average); and 3) unusually weak winds and currents in the Western Basin of Lake Erie (WBLE) in late winter and spring, leading to poor mixing and longer residence times than in previous years, and thus less dilution and flushing of nutrients from the system. During the 2011 bloom, *Microcystis* sp. depleted the N pool and was replaced by a secondary bloom of N_2-fixer *Dolichospermum* sp. It is unclear how nutrient loading, weather patterns, and recurring cyanobacterial blooms interact to influence the seasonal succession of other phytoplankton taxa which may be particularly important for supporting production at higher trophic levels.

Seasonal patterns of phytoplankton community succession depend upon environmental conditions, nutrient supply, competition among phytoplankton species, and herbivory. The Plankton Ecology Group hypothesized that these processes create a predictable seasonal

succession in phytoplankton communities, mediated by climate, herbivory, as well as by the loading of nutrients and suspended sediments (Sommer et al. 1986, Sommer et al. 2012). Yet, these seasonal dynamics are poorly documented for shallow, riverine-dominated systems such as the WBLE (Briland 2018).

It is not clear whether spring phytoplankton dynamics in WBLE follow the predictions of Sommer et al. (1986). Sommer et al. (1986) predict that small, fast growing diatoms and green algae should dominate in the spring when water temperatures are relatively cool, nutrient and Si concentrations are high, and herbivory is relatively low. Yet spring Maumee River plumes in the WBLE—which deliver growth-fueling nutrients as well as sediments that rapidly attenuate light—may alter these hypothesized dynamics in hard to predict ways by altering the resource environment (i.e., nutrient and light availability).

Sommer et al. (1986) predicted that herbivore-resistant taxa that are effective competitors for nutrients would dominate in the mid- to late summer. Consistent with this prediction, high N and P loading to WBLE has led to predictable blooms of *Microcystis* (Chaffin et al. 2011, Bridgeman et al. 2012, Stumpf et al. 2016, Ho and Michalak 2017) which has high temperature requirements and is an effective competitor for nutrients (Paerl et al. 2011). In many years, the *Microcystis* sp. bloom is followed by an increase in N_2-fixer *Dolichospermum* sp. (Michalak et al. 2013, Watson et al. 2016). Herbivory is predicted to play an important role in shaping phytoplankton succession (Sommer et al. 1986, Sommer et al. 2012); however, the relative importance of herbivory in WBLE with its strong bottom-up and top-down controls is poorly understood (but see: Boegman et al. 2008, Zhang et al. 2016).

We lack a comprehensive understanding of how environmental and biotic factors contribute to phytoplankton community dynamics in WBLE which impedes the management of this system. Over the last twenty years, the WBLE has experience increases in precipitation in its watershed and nutrient loading (Baker et al. 2014a, Stow et al. 2015), changes in the abundances of non-native taxa, but not directional changes in water temperature (Mason et al. 2016, Zhong et al. 2018). It is unclear how these changing patterns of precipitation, biotic invaders, and nutrient loading have interacted with other physiochemical factors (e.g., water temperature) to alter the relationship between phytoplankton community dynamics and key physiochemical and biological drivers (i.e., a regime shift; Yuan et al. 2014). Furthermore, while understanding the controls on bloom forming species is critical, it is important to look beyond these taxa and understand the dynamics and mechanistic drivers of other phytoplankton groups (e.g., green algae, diatoms, and cryptophytes). In particular, the influence of climate and nutrient

loading on edible phytoplankton taxa, which likely fuel food web production, has received little attention (but has been addressed in lake models: Zhang et al. 2008, Kane et al. 2009, Roy et al. 2010).

Managing environmental resources in the face of a highly variable environment with directional change in key physiochemical drivers requires monitoring as well as a mechanistic understanding, rooted in ecological theory, of the important drivers of those dynamics. Luckily, in WBLE abiotic and biotic monitoring data exists which can be used to identify trends and develop generalizable predictions of community-wide response to nutrient enrichment and warming at both intra- and interannual time scales. These data can also be used to characterize the dependence of key species or functional groups on the physiochemical environment as well as their interactions (Ives et al. 2003, Hampton et al. 2008, Hampton et al. 2013). Given the extensive monitoring of phytoplankton dynamics in WBLE, we possess the necessary data and statistical tools to gain a much more comprehensive understanding of the rapid ecological change underway in the WBLE.

Here, we ask how climate and nutrient loading have interacted to shape WBLE phytoplankton dynamics on both an intra- and interannual temporal scale. We analyzed the 20-year Lake Erie Plankton Abundance Survey time series (LEPAS, Fig. 1) using a combination of univariate and multivariate statistical modeling approaches (Fig. 2). We have split this analysis into two components which separately emphasize temporal or spatial variation. Our first manuscript focuses on phytoplankton dynamics at one site near the mouth of the Maumee River which likely typifies phytoplankton responses to terrestrial nutrient and sediment subsidies. The second manuscript will examine phytoplankton community patterns across all eight LEPAS sites in the WBLE. This research, which is ongoing due to issues associated with recruiting and retaining postdoctoral associates, will elucidate how climatic variability and changes in the timing and magnitude of nutrient loading have led to shifts in the phenology and strength of biotic responses of both bloom-forming cyanobacteria and other phytoplankton taxa during a 20-year period of rapid environmental change.

Methods

Datasets

We combined three datasets for these analyses (Fig. 2): phyto- and zooplankton data from the LEPAS program, nutrient loading data from the Heidelberg University National Center

for Water Quality Research (NCWQR), and Maumee River discharge data the United States Geological Survey (USGS; Station 04193500). Permissions associated with those datasets are described in the original grant application (SG-531-2018).

The Lake Erie Plankton Abundance Survey (LEPAS, Ohio Department of Natural Resources Division of Wildlife and The Ohio State University) is a 20-year (1995-2015) dataset that includes information on phytoplankton and zooplankton community biomass, water temperature, and dissolved oxygen from eight sites in the WBLE (Fig. 1; Kane et al. 2014). Samples were collected approximately biweekly from May through September, and phytoplankton are enumerated to genus while zooplankton are enumerated to species for common taxa and to Phyla or Family for rare taxa (Briland 2018). To analyze the relationship between phytoplankton abundances and nutrient (N, P and Si) loadings from the Maumee river, we have augmented this dataset with USGS discharge data for the Maumee River (Station 04193500), and with solute and nutrient data for the Maumee River from NCWQR. Discharge and solute chemistry data are provided at a daily or sub-daily resolution for the majority of the period between 1995 and 2015. These data include discharge (Q), total phosphorus (TP), dissolved reactive phosphorus (DRP), nitrate (NO_3), total nitrogen (TN) and dissolved silica (Si). Analytical methods used to derive these data are described in depth elsewhere (Baker et al. 2014a). Dr Laura Johnson (NCWQR) provided daily estimates of TN, TP, DRP, and dissolved Si loads from the Maumee River into Lake Erie for the 1995-2015 period, which were calculated following the NCWQR's standard protocol (Baker et al. 2014a). Baker et al. (2014a) showed that the total bioavailable fraction of phosphorus (TBP) includes ~26% of the total particulate phosphorus (TPP), and TBP is thus preferable to DRP for predicting phytoplankton responses (see also: Stumpf et al. 2016). TBP is calculated as

$$TBP = [(TPP - DRP) \times \phi \times (1 - S)] + DRP \qquad (1),$$

where ϕ is the fraction of TPP that is bioavailable and S is the fraction of TPP that is lost to settling (Stumpf *et al.* 2016). We used TBP instead of DRP in all models and calculations.

In the first manuscript (Fig. 2), we explored relationships between Maumee River nutrient loads and phytoplankton community dynamics at a single sampling location in the Western Basin of Lake Erie, near the mouth of the Maumee River (site # 36-873; 41° 44' 27.999" N; 83° 20' 31.999" W). Of all the LEPAS sampling sites, this site experiences the earliest and most direct exposure to Maumee River discharge, and may be a bellwether for other, offshore sites.

An underemphasized question in research that attempts to link riverine nutrient loads with lake phytoplankton community dynamics is: Over what time scale or scales do nutrient loads shape phytoplankton community dynamics? For the WBLE, there is clear evidence that nutrient loads integrated over both short- and long-time periods shape phytoplankton community dynamics (Stumpf et al. 2016, Ho and Michalak 2017). The directional impacts of loads integrated over these windows may differ in sign. For instance, sediment in riverine plumes might negatively impact phytoplankton due to shading over short periods while associated nutrient loading would contribute to an increase in phytoplankton biomass over longer periods. In our preliminary analyses, we evaluated a wide variety of loading windows ranging from one to 365 days. Many of these loading windows were strongly correlated ($r > 0.7$); so, we focused on one short-term and one long-term metric of loading. We calculated short-term loads integrated over the 14 days preceding the sampling date (henceforth "14-day"). Following Stumpf *et al.* (2016), long-term loads were the sum of nutrient loads from March through July, or up to the sampling date, whichever came first (hereafter "Spring"). The Maumee River discharge data we used were collected at a site near Watersville, OH which we estimated was approximately 5 days of water travel time from our focal site near the Maumee River mouth (also see: Baker et al. 2014b). Thus, nutrient loading rate for the 14-day window for a phytoplankton sample on 1 June 2019 would be the sum of nutrient loads from 13 May 2019 to 27 May 2019 (a 5-day lag).

Statistical analyses

Phytoplankton community structure and dimension reduction (Maumee Site manuscript)

Our first question for the Maumee Site manuscript was, which taxa are the major players in WBLE phytoplankton communities and how have those communities changed over time? To address that question, we used a principal coordinate analysis (PCoA) to reduce the dimensionality of the phytoplankton dataset and to facilitate interpretation of "big-picture" changes in phytoplankton community structure resulting from the large *Microcystis* sp. blooms that began in the early 2000s. As it has been shown that large summer *Microcystis* sp. blooms have been occurring since about 2003 (Scavia *et al.* 2014), we conducted separate analyses on pre-bloom years (1995-2002) and bloom years (2003-2015) to determine how community structure was affected by the onset of extreme bloom events. This decision was also supported by preliminary analyses. Phytoplankton taxa were included in the PCoA at the highest available taxonomic resolution, typically genus; however, only taxa that had greater than 1% of the total

biomass in at least one sample were included in the analysis to avoid overrepresenting the effects of rare species. Our PCoA, conducted using the "vegan" R package version 2.5-4 (Oksanen *et al.* 2018), condensed taxonomic variation into two axes based on Bray-Curtis dissimilarity indices. This facilitated visual interpretation of the phytoplankton abundance data and simplified later statistical modeling: we identified the taxa with the top 4 scores related to each PCoA axis (typically |score| ≥ 0.5) as important taxa to be addressed in the GAMM and MARSS models described below.

Temporal variation of phytoplankton biomass (Maumee Site manuscript)

Our second question in the Maumee Site manuscript had two components: (1) what is the characteristic seasonal dynamics of key phytoplankton groups in WBLE and (2) has the timing of those seasonal dynamics changed over the period of record? We used generalized additive mixed models (GAMMs) to address these questions and several others for this project. GAMMs are preferable to linear models when the relationships being modeling are nonlinear, which is commonly the case for phytoplankton phenology and the relationship between phytoplankton biomass and key physiochemical drivers (e.g., temperature or resource availability).

To address these questions, we modeled the biomasses of important phytoplankton taxa (identified by the PCoA above) and several abiotic predictors as functions of year, week-of-year (WOY) and WOY × year interactions. The model is as follows:

$$Y \sim f(week_t) + f(year_t) + f(week_t * year_t) + \varepsilon_t;$$
$$\varepsilon_t \sim N(0, \sigma^2); \qquad (1),$$
$$cor(\varepsilon_s, \varepsilon_t) = \rho^{|t-s|}$$

where Y is the biomass of the target phytoplankton group, f is a smoother for each covariate (Wood 2006), and ε_t is the error term allowing for temporal autocorrelation of errors. Temporal autocorrelation is implied in the model by the third part of phenological model above, in which ρ is the correlation coefficient and s is any year except year t; thus $|s - t|$ is larger when two years are farther apart in time. For many phytoplankton biomasses, a Gamma distribution provided a superior fit to a Gaussian distribution, due to zero inflation. The exceptions to this were cyanobacteria and *Aulacoseira* sp. biomass, which had to be fit using *log(y+1)*-transformed biomass data with a Gaussian distribution due to convergence failure with the Gamma distribution. We tested for autocorrelation by building models with and without an

ARMA(1,0) residual structure of WOY nested in year to account for seasonal and annual autocorrelation and then comparing AIC values for each (Zuur et al. 2017). All models had lower AIC values with the residual autocorrelation structure, so we continued using it in the models.

We interpreted phenological models in the following way. A significant value for WOY indicated that the taxa had a seasonal pattern throughout the ice-free season. A significant value for year indicated that there was annual change in the biomass of the taxa. If both WOY and year were significant, but the interaction was not, then the seasonal pattern was becoming more or less intense annually, but not shifting during the season. Finally, a significant WOY*year interaction indicated a shift in the seasonal pattern changing in duration or developing new peaks. GAMM analyses were performed using the “mgcv” package in R (Wood 2019).

Mechanistic controls of phytoplankton community dynamics (Maumee Site manuscript)

Next in the Maumee Site manuscript, we examine the dominate physiochemical and biological drivers of phytoplankton dynamics. We used GAMM models to identify how the dynamics of groups of similar phytoplankton taxa (represented by the two PCoA axes described above) are shaped by wind speed and direction, Maumee River discharge, nutrient loadings, nutrient ratios, water temperature, and total zooplankton biomass. Preliminary analysis indicated that wind speed or direction had little explanatory power. We initially included an ARMA(1,0) autocorrelation structure in these models to account for temporal autocorrelation across years, but found that inclusion of this correlation structure did not improve models (dAIC = 2 with 2 df). The form of the model used is as follows:

$$PCoA\ Axis \sim f(X_1) + f(X_2) + \cdots + f(X_n) + \varepsilon$$
$$\varepsilon \sim N(0, \sigma^2) \qquad (1),$$

where $X_1 \ldots X_n$ represent n predictors, f indicates a nonlinear smoother for each covariate and ε is the error term. Final model parameters and (lack of) autocorrelation structure were determined by a step-backward approach, using AIC for model comparisons (Zuur et al. 2009). The most likely models were checked for heterogeneity and normality by examining the normalized residuals of the model fit against each predictor (Zuur et al. 2009). The predictors included in the final model are shown in Table 3 of the Results. For each predictor, a significant effect on PCoA Axis 1 can be interpreted primarily as an effect on cyanobacterial biomass, while a positive effect on Axis 2 can be interpreted as a positive effect on diatom biomass and a

negative effect on green algae and cryptophyte biomass. To determine the relative importance of each predictor in the mechanistic driver models (i.e. the amount of variation in each PCoA Axis that was explained by each predictor), we fit a separate model with only the single covariate of interest ($Axis \sim f(X_n) + \varepsilon$), and calculated the adjusted R^2 value of that model (Cox et al. 2017).

Community and food web interactions (Maumee Site manuscript)

Our final question in the Maumee Site manuscript asks how physiochemical and biotic interactions (both herbivory and competition) shapes the dynamics of key phytoplankton taxa? To address this question we used multivariate autoregressive state-space models (MARSS) which leverage time series data to quantify the strengths and directions of interactions among multiple entities in a system (Ives *et al.* 2003, Holmes *et al.* 2012, Hampton *et al.* 2013). By simultaneously incorporating density-dependent interactions among biota, linear relationships between biota and key covariates, measurement errors and autocorrelation of process errors in time, MARSS models are a powerful means of characterizing an interaction web such as an ecological community. Using the "MARSS" R package (Holmes et al. 2018), we are currently refining MARSS models that integrate climate, nutrient and river discharge data with abundances of several key phytoplankton and zooplankton taxa from the 20-year LEPAS dataset, with the ultimate objective of obtaining the most comprehensive understanding to date of how climate, nutrients, competition, and herbivory interact to produce the phytoplankton dynamics we have observed in the western basin of Lake Erie over the past 20 years. Such models have been used to great effect on time series data from other systems in the past (Hampton *et al.* 2006, Hampton et al. 2008), and are among the best statistical tools available for understanding how the components of an ecosystem interact and change over time.

Spatial-temporal modeling of phytoplankton dynamics (Spatial Patterns manuscript)

Our primary question in the Spatial Patterns manuscript is: How do the mechanistic linkages between key phytoplankton taxa and physiochemical and biotic drivers influence spatial patterns in phytoplankton community structure? To address this question, we used spatially- and temporally-explicit generalized additive models (GAMs) to predict biomass dynamics of broad phytoplankton taxonomic groups (cyanobacteria, diatoms, green algae, and cryptophytes) across the WBLE using the INLA R package version 3.5.1 (Rue et al. 2009,

Lindgren et al. 2011). These models are currently in revision. Briefly, we used these models to characterize the spatial distribution of each taxonomic group in pre-bloom (1995-2002) and bloom (2003-2015) time periods. These models use Bayesian integrated nested Laplace approximations (INLA) to extrapolate the biomass of each taxon to nodes on a triangulated mesh spread across the study area (Zuur et al. 2017, Zuur and Ieno 2018). The models use random spatial intercepts (u), a random effect of year (a), and a non-linear fixed effect of day of week, $s(DOW)$, to predict the log-transformed biomass of each group.

$$\log(Biomass) = Intercept + s(DOW) + a + u + \varepsilon$$

$$a \sim N(0, \sigma^2_{Year})$$

$$\varepsilon \sim N(0, \sigma^2)$$

$$u \sim GMRF(0, \Sigma)$$

This model assumes normally distributed errors with mean 0 and variance σ^2, with independently distributed random effects for each year with mean 0 and σ^2_{Year}. The random spatial intercepts (u) are assumed to be spatially correlated with the mean (0) and the covariance matrix (Σ) (Zuur et al. 2017). We used a Gaussian Markov random field (GMRF) to extrapolate the u, assuming that they are normally distributed and that only observations from adjacent sites are correlated. A continuous domain partial stochastic differential equation (SPDE) is used to calculate the values of the nodes in the GMRF mesh and their covariance matrix (Zuur et al. 2017, Zuur and Ieno 2018).

Results

Maumee site manuscript

Phytoplankton community structure

The principle coordinates analyses (PCoA) revealed both an increase in cyanobacteria blooms between 2003 and 2015, consistent with other datasets, as well as a surprisingly strong continuity in the structure of the non-cyanobacteria phytoplankton community (Fig. 3). In this PCoA, variation along Axis 1 was strongly correlated with cyanobacteria relative abundance, specifically *Microcystis* sp. (Cyanophyceae). Diatoms were positively correlated with Axis 2 while green algae and the common cryptophyte *Chroomonas* sp. were negatively correlated with Axis 2. Between 1995 and 2002 phytoplankton communities were dominated by diatoms, green algae, and cryptophytes while between 2003 and 2015 phytoplankton communities were

often dominated by cyanobacteria (rightward shift of points in Fig 3b), but also had frequent periods during which diatoms, green algae, and cryptophytes dominated the phytoplankton community (negative PCoA Axis 1 values in Fig 3).

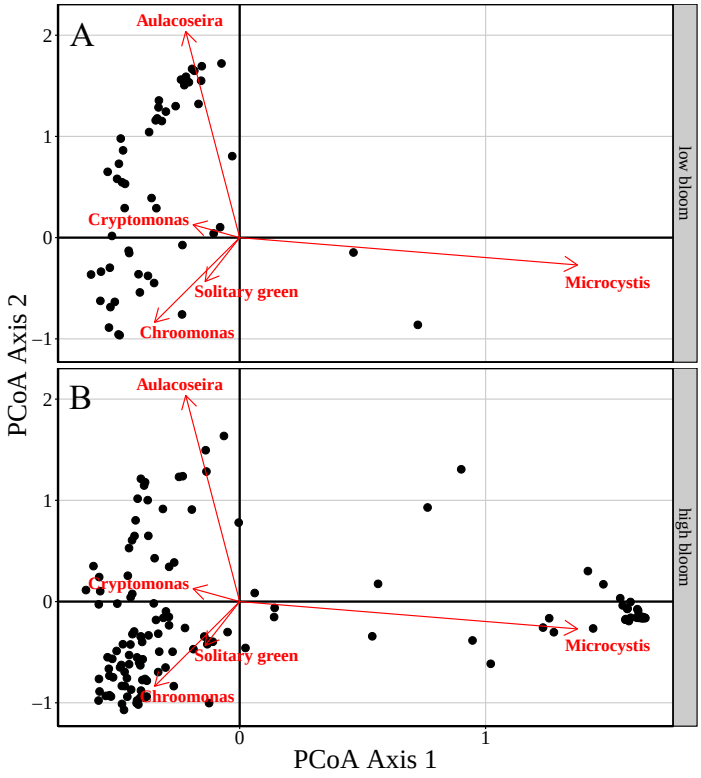

Figure 3. Principle coordinates analysis of phytoplankton biomass by taxon (n = 56 taxa) during (A) 1995-2002 and (B) 2003-2015. Variation in PCoA Axis 1 is strongly correlated with cyanobacteria relative abundance, while Axis 2 is positively correlated with diatoms and negatively correlated with green algae and the cryptophyte *Chroomonas* sp. Each point is a sampling occasion at the site closest to the Maumee River. For correlations between Axes 1, 2 and the five taxa shown in red, see Table 1.

Table 1. Correlations between PCoA Axes 1 & 2 and the five phytoplankton taxa most influential of those axes (shown in red in Figure 3).

Taxon	Axis 1	Axis 2
Aulacoseira sp.	0.23	0.37
Chroomonas sp.	0.04	-0.29
Cryptomonas sp.	0.03	0.07
Microcystis sp.	0.36	-0.03
Solitary greens	<-0.01	-0.12

Temporal variation in phytoplankton biomass

Mean annual biomass of cyanobacteria, diatoms, cryptophytes, and green algae all clearly increased between 1995 and 2003 (Figure 4), however GAMMs were able to more precisely capture seasonal changes (*week* effect), interannual changes (*year* effect) and changes in seasonal trends over time (*week* × *year* interaction) in the biomass of each broad taxonomic group (Figure 5, Table 2). Between 1995 and 2015, cyanobacterial biomass was characterized by a late summer/fall bloom that has been increasing in intensity and becoming longer in duration throughout the time series (*week* × *year*, $P < 0.0001$; Figure 5A; 2).

Diatoms exhibited a phenological shift: the spring peak that is apparent early in the time series shifts later and increased in magnitude over time, becoming a mid-late summer bloom, peaking in August (*week* × *year*, $P = 0.0046$; Figure 5B; Table 2). Neither cryptophytes nor green algae exhibited a detectable seasonal pattern throughout the time series (*week*: $P_{cryptophytes} = 0.14$; P_{greens} 0.80; Figure 5C,D; Table 2). However, both groups saw an increase in biomass between 1995 and 1999, at which point the biomass remained constant (*year*: $P_{cryptophytes} < 0.0001$; $P_{greens} < 0.0001$; Figure 5C,D; Table 2).

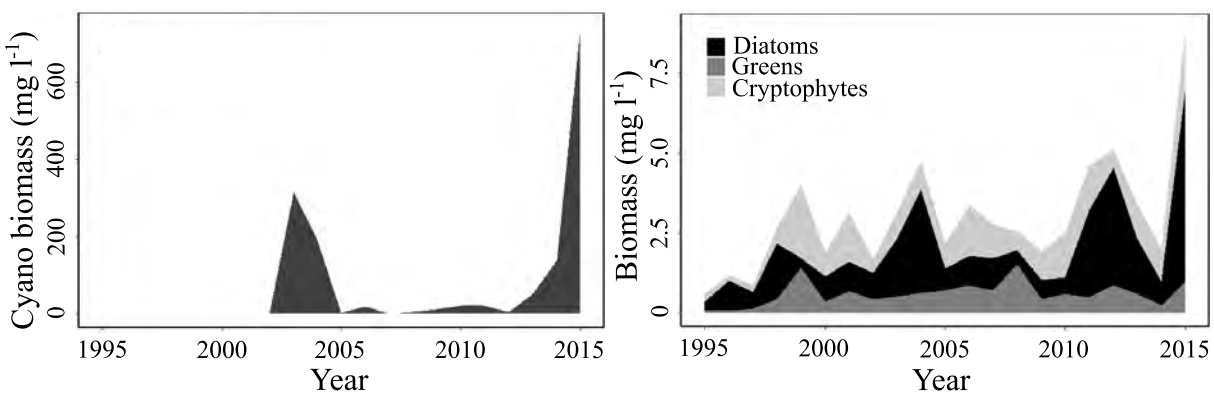

Figure 4. Trends in mean annual A) cyanobacteria and B) diatoms, green algae, and cryptophytes biomass between 1995 and 2015. Note differences in y-axis scales.

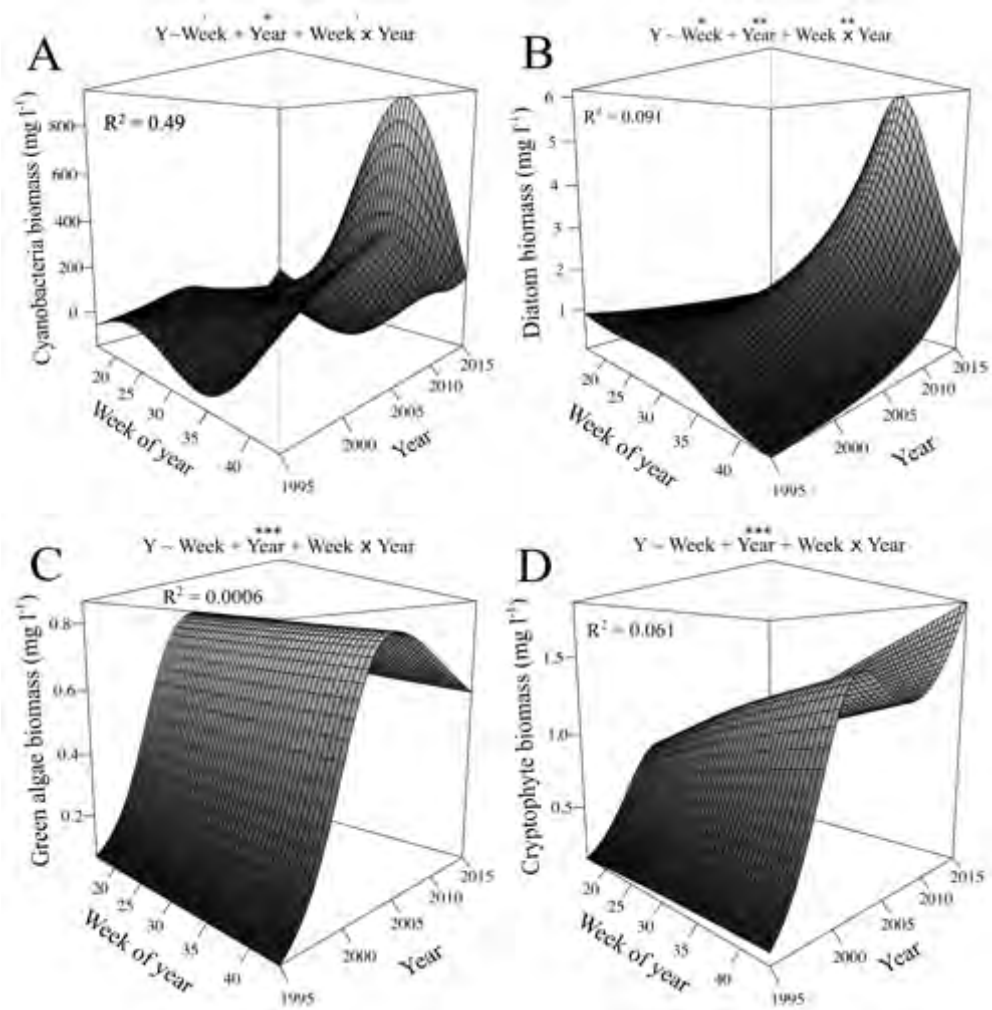

Figure 5. GAMM smoother interaction surfaces showing the fitted values for A) *log(y+1)*-transformed cyanobacteria biomass, B) diatom biomass, C) green algae biomass, and D) cryptophyte biomass as functions of year and week-of-year.

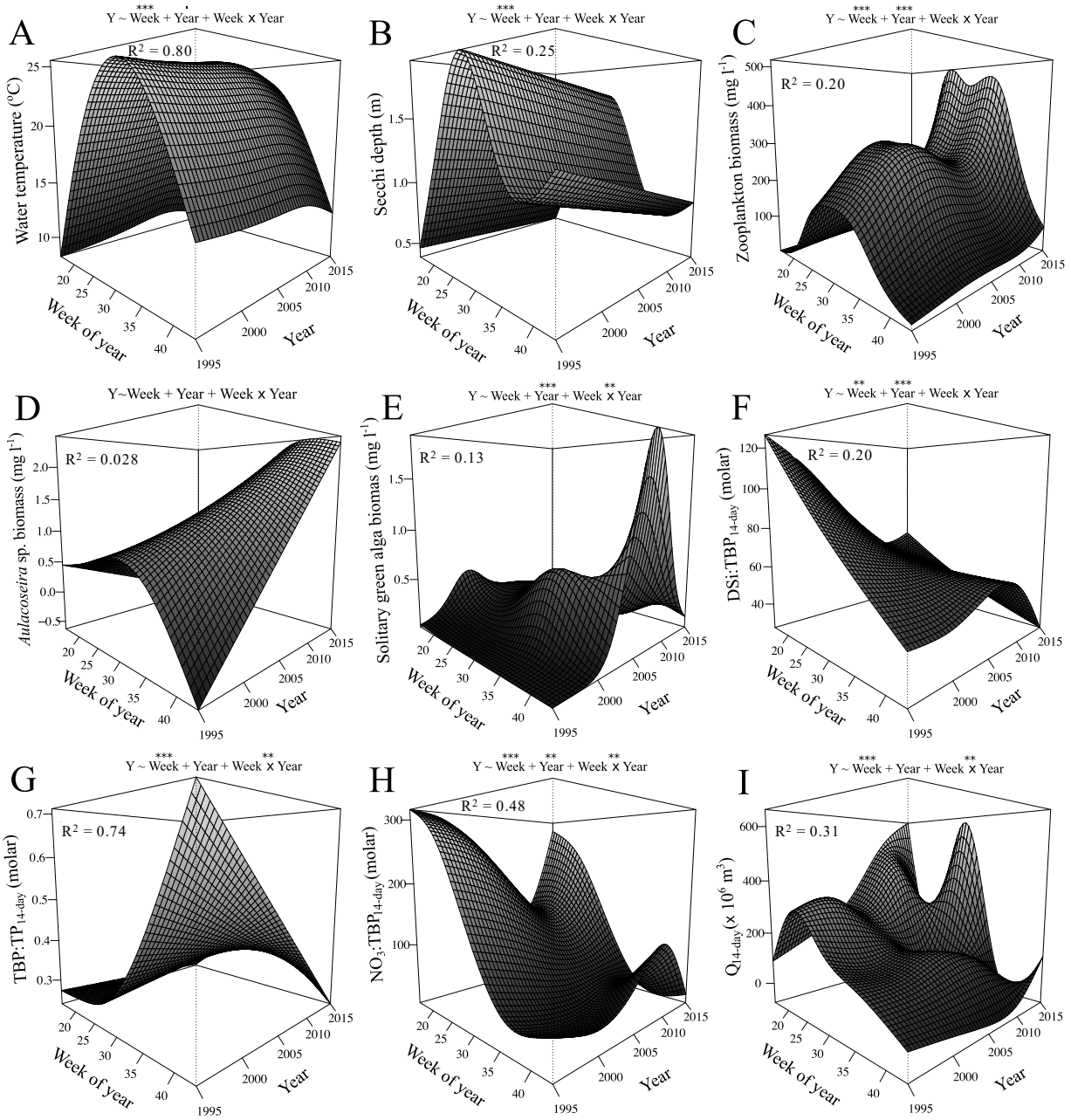

Figure 6. GAMM smoother interaction surfaces showing intra- and interannual variation in the covariates used in the mechanistic models, each as a function of year and week-of-year. Smoothing function for A) instantaneous water temperature; B) Secchi depth; C) Zooplankton biomass; D) *Aulacoseira* sp. biomass; E) Solitary green algae biomass; F) 14-day DSi:TBP loading ratio; G) 14-day TBP:TP loading ratio; H) 14-day NO_3:TBP loading ratio; and I) 14-day integrated Maumee River discharge.

Table 2. Results of GAMMs examining intra- and interannual variation in biomass of cyanobacteria, diatoms, green algae and cryptophytes as well as in the covariates used in the mechanistic models (see Table 3). Covariate models are shown to summarize intra- and interannual patterns in the covariate data used in these analyses and should not be used to evaluate patterns of change in these parameters due to the way they were subsampled or summarized for these models. For instance, models of 14-day TBP:TP loading, which indicate no interannual pattern in this loading ratio over time, should not be interpreted as indicating that TBP:TP loading ratio to WBLE has not changed between 1995 and 2015. R^2 is the proportion of variation in the indicated response variable captured by the whole model. For definitions and exceptions see bottom of table.

Model	P_{Week}	P_{Year}	$P_{Week \times Year}$	**AIC**	R^2
Biomass models					
Cyanobacteria (mg l^{-1})*	**<0.001**	**<0.001**	**<0.001**	645	0.490
Diatom (mg l^{-1})	**0.018**	**0.005**	**0.009**	732	0.091
Greens (mg l^{-1})	0.800	**<0.001**	0.950	708	< 0.001
Cryptophytes (mg l^{-1})	0.140	**<0.001**	0.820	532	0.061
Significant covariate models					
Water Temp (°C)	**<0.001**	0.091	0.210	742	0.800
Secchi depth (m)	**<0.001**	0.130	0.620	378	0.250
Zooplankton biomass (mg l^{-1})	**<0.001**	**<0.001**	0.250	496	0.200
Aulacoseira sp. biomass (mg l^{-1})*	0.092	0.400	0.060	352	0.028
Solitary Green biomass (mg l^{-1})	0.500	**<0.001**	**<0.001**	583	0.130
$DSi:TBP_{14\text{-day}}$ (molar)	**0.002**	**<0.001**	0.160	1737	0.200
$TBP:TP_{14\text{-day}}$ (molar)	**<0.001**	0.550	**0.007**	-757	0.740
$NO3:TBP_{14\text{-day}}$ (molar)	**<0.001**	**0.005**	**0.003**	2083	0.480
$Q_{14\text{-day}}$ (10^6 m^3)	**<0.001**	0.160	**0.001**	2412	0.310

Definitions: P_{Week}: P-value for Week-of-year effect; P_{Year}: P-value for Year effect; $P_{Week \times Year}$: P-value for interaction effect. **14-day**: as in Figure 2.

* Biomasses of starred taxa were *log(y+1)*-transformed and fit assuming a Gaussian distribution. All other phytoplankton taxa and physical covariates were fit assuming a Gamma distribution with a log link function.

Temporal variation in Western Basin biota, physio-chemistry, and loading

Most of the significant physio-chemical predictors of PCoA Axes 1 and 2 (Model 1) varied at both intra- and interannual scales, and several exhibited notable changes in seasonal trends between 1995 and 2015 (Figure 6; Table 2). Water temperature and Secchi depth varied seasonally, but did not differ among years (Figure 6A, B; Table 2). Zooplankton biomass varied seasonally and changed significantly from year to year, but seasonal trends in zooplankton biomass did not shift. *Aulacoseira* sp. biomass did not vary seasonally or interannually, but there was a marginal shift from early- to late-summer blooms. Solitary green algae did not exhibit a main effect of week-of-year but bloomed regularly in late summer between 2003 and 2010 (Figure 6E; Table 2). 14-day river discharge ($Q_{14\text{-day}}$) and three nutrient loading ratios ($DSi:TBP_{14\text{-day}}$, $TBP:TP_{14\text{-day}}$, $NO3:TBP_{14\text{-day}}$) varied significantly at the intra-annual scale, however there were no main effects of *year* on $TBP:TP_{14\text{-day}}$ and $Q_{14\text{-day}}$. $Q_{14\text{-day}}$, $DSi:TBP_{14\text{-day}}$ decreased significantly between 1995 and 2015. These short-term loading ratios and rates are not correlated with annual loading rates or ratios. $TBP:TP_{14\text{-day}}$, and $NO3:TBP_{14\text{-day}}$ showed significant changes in seasonal trends between 1995 and 2015, with $NO3:TBP_{14\text{-day}}$ exhibiting a late-summer peak around 2010, but not in earlier or later years (Figure 6; Table 2).

Table 3. Significant predictors of PCoA Axis 1 and/or Axis 2 used in the mechanistic GAMM models. The "--" in place of a number symbol indicates that a given predictor is not a significant predictor of that PCoA axis. Each adjusted R^2 is from a GAMM fit to PCoA Axis 1 or 2 as a function of that predictor alone and thus indicates the contribution of that covariate to the most likely model. Mean ± sd are overall means and standard deviations of predictors. For all other definitions, see bottom of table.

		PCoA Axis 1 model			PCoA Axis 2 model		
Variable	**Mean ± sd**	**edf**	**P**	**adj R^2**	**edf**	**P**	**adj R^2**
Water (physical)							
Water temp. (°C)	21.25 ± 4.07	1.00	**0.006**	0.064	1.99	**0.032**	0.049
Secchi depth (m)	1.29 ± 0.76	1.00	**<0.001**	0.003	--	**--**	--
Community biomass (mg l^{-1})							
Zooplankton	213.03 ± 199.8	1.00	0.110	0.080	--	**--**	--
Aulacoseira sp.	1.08 ± 3.20	1.00	**0.003**	0.090	3.53	**<0.001**	0.560
Solitary green	0.23 ± 0.32	1.00	**0.025**	0.004	2.05	**0.007**	0.170
Nutrient loading and river discharge							
$DSi{:}TBP_{spring}$	65.62 ± 19.90	3.18	**<0.001**	0.083	1.00	**0.019**	0.038
$NO3{:}TBP_{spring}$	131.75 ± 60.82	--	**--**	--	1.00	**<0.001**	0.091
$NO3{:}TBP_{14\text{-}day}$	116.40 ± 35.49	1.00	**<0.001**	0.160	--	**--**	--
$TBP{:}TP_{spring}$	0.28 ± 0.050	2.72	**<0.001**	0.140	2.29	**0.002**	0.110
$Q\ (10^6\ m^3)_{spring}$	2784 ± 1208	--	**--**	--	1.00	0.130	0.007
$Q\ (10^6\ m^3)_{14\text{-}day}$	197.9 ± 244.02	1.00	**<0.001**	0.055	--	--	--
$DSi{:}TBP_{spring} \times Q_{spring}$	--	1.00	**0.020**	0.210	--	--	--
$NO3{:}TBP_{spring} \times Q_{spring}$	--	--	--	--	1.00	**<0.001**	0.14

Definitions: sd: standard deviation; **edf**: estimated degrees of freedom consumed by smoother; **P**: P-value; **adj. R^2**: adjusted R^2, i.e. proportion of variation in the response variable explained by a single predictor; ; **spring**: sum of indicated variable for March through July of each year; **14-day**: 14-day sum of discharge or nutrient loading ratio, lagged by 5 days to account for travel time down the Maumee River.

Mechanistic controls of phytoplankton community structure

PCoA Axis 1: cyanobacteria

The most likely model of PCoA Axis 1, in which positive values indicate cyanobacteria-dominated communities, contained covariates describing nutrient loading and river discharge, lake temperature and transparency, as well as several biotic predictors (adj R^2 = 0.89, Fig. 7, Table 3). Taken together, covariates associated with riverine discharge (Q) and nutrient loading ratios explained 64.8% of the variation in PCoA Axis 1. The most important riverine covariates contributing to this model were: $TBP:TP_{14\text{-}day}$, $NO_3:TBP_{14\text{-}day}$, and a $DSi:TBP_{spring} \times Q_{spring}$ interaction (Table 3). In general, these coefficients conspired to create a positive relationship between cyanobacteria biomass and TBP loading. Yet, each of these loading ratios were better predictors than TBP loading alone.

Both spring and 14-day integrated covariates played an important role in this model. Spring loading covariates explained more variation in this model than 14-day integrated covariates (spring = 43.3%; 14-day = 22%). The most important spring variable was the $Q_{spring} \times DSi:TBP_{spring}$ interaction. Cyanobacteria biomass generally increased with Q_{spring} (Maumee River discharge) and was unimodally related to $DSi:TBP_{spring}$ with a maximum at ~55 (Fig. 7I). Similarly, cyanobacteria biomass exhibited a U-shaped relationship with $TBP:TP_{spring}$ (Fig. 7G). Cyanobacteria blooms declined with $TBP:TP_{spring}$ up to a ratio of ~0.25 and then began to increase with increasing $TBP:TP_{spring}$. Cyanobacteria also declined with $NO_3:TBP_{spring}$, the most important 14-day integrated variable (Fig. 7F, Table 2), and $Q_{14\text{-}day}$ (Fig. 7H). The decline of cyanobacteria relative abundance with $Q_{14\text{-}day}$ likely reflects the influence of shading by riverine sediments or flushing by Maumee River waters.

Cyanobacteria biomass increased with instantaneous water temperature (~6.4% of variation in PCoA Axis 1; Fig 7A). There appears to be a threshold in the data above 20°C which the model did not capture, suggesting that bloom might be associated with temperatures greater than 20°C. The biomass of zooplankton and the diatom *Aulocoseira* sp. both made significant contributions to the model, explaining nearly 10% of the variation each (Fig. 7 C and D, respectively). Surprisingly, cyanobacteria biomass increased with zooplankton biomass, although the spread around the fit was considerable. Cyanobacteria biomass also increased with *Aulacoseira* sp. biomass, although this pattern was driven by a dozen sampling dates on which *Aulacoseira* sp. biomass was relatively high.

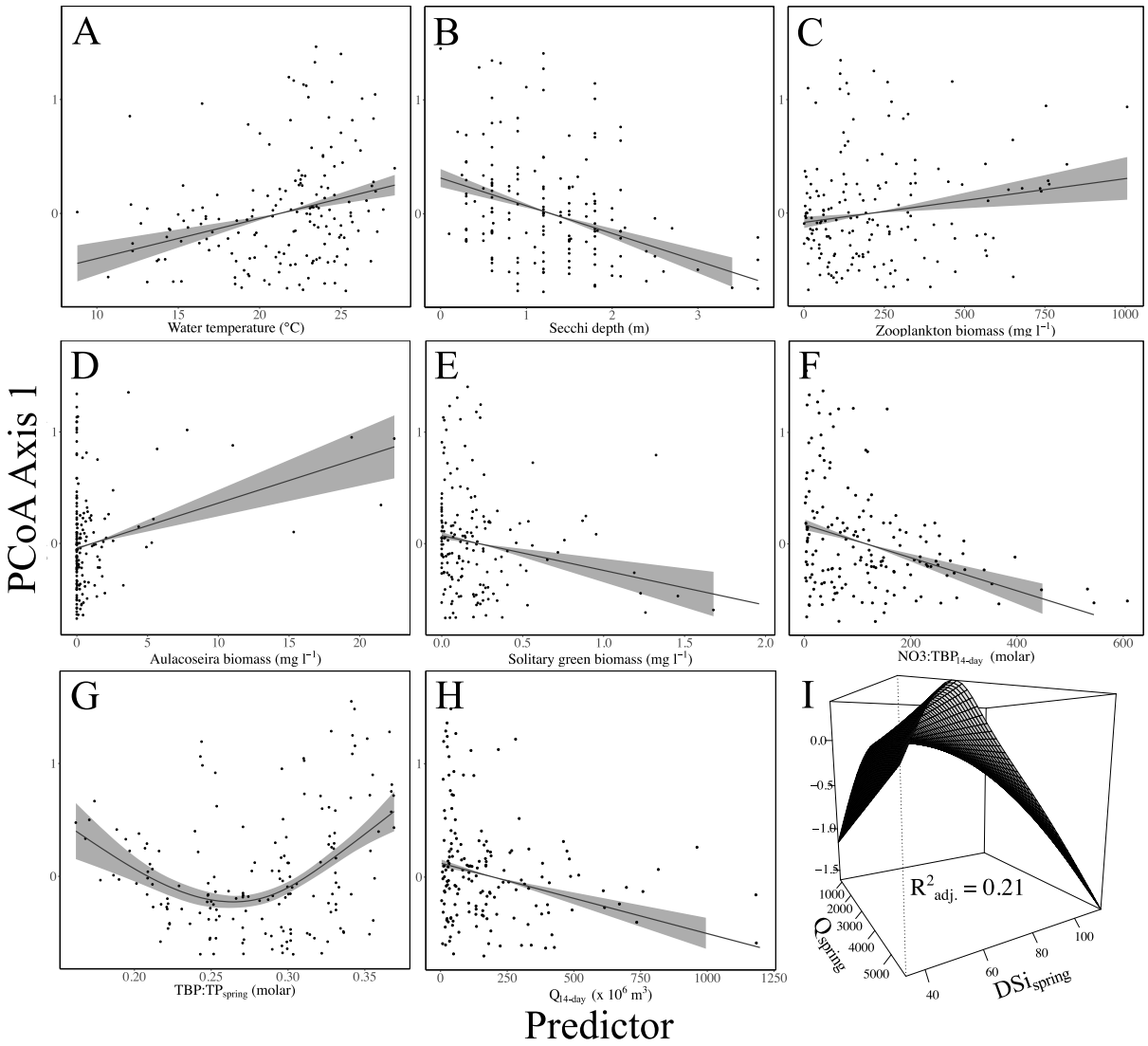

Figure 7. Panels A-I show estimated smoothing curves or surfaces for 10 predictors of PCoA Axis 1 mechanistic model. PCoA Axis 1 was positively correlated with cyanobacterial relative biomass. The predictors are on the *x*-axis, and the curves show the contribution of the smoother to the fitted values. “Spring” and “14-day” indicate the period for which data are integrated, as described in Methods. Bands are ±1 SE. Points are the fitted model + residuals. In I, the response surface is the smoother for the $Q_{spring} \times DSi{:}TBP_{spring}$ interaction.

PCoA Axis 2: green algae, diatoms, and cryptophytes

Species loading onto PCoA Axis 2 was considerably more complex than PCoA Axis 1. Biomass of *Aulacoseira* sp. and solitary green algae were the strongest predictors of PCoA Axis 2, explaining 73% of the variation in this axis (Fig. 8, Table 3). In general, the diatom *Aulacoseira* sp. was most common when PCoA Axis 2 was high while the solitary green group was high when this Axis was low. Both of these relationships were non-linear. PCoA Axis 2 increased rapidly with *Aulacoseira* sp. biomass and then plateaued (Fig. 8B). In contrast, PCoA Axis 2 exhibited a weak U-shaped relationship with solitary green biomass (Fig. 8C). Zooplankton biomass was not included in the most likely model.

The most important non-biotic predictors of PCoA Axis 2 were spring integrated nutrient loading ratios and river discharge related variables including: NO_3:TBP_{spring} × Q_{spring}, TBP:TP_{spring}, and NO_3:TBP_{spring}. The NO_3:TBP_{spring} × Q_{spring} interaction explained the largest proportion of variability out of this group (14%) and indicated that high NO_3:TBP_{spring} ratios favored diatoms, particularly following wet springs. This interaction could be interpreted to indicate that high NO_3 loading benefited diatoms, particularly *Aulacoseira* sp. PCoA Axis 2 declined nonlinearly with TBP:TP_{spring} indicating that low TBP:TP loading ratios in the spring favored diatoms. A phenomenon which was common before 2003 (also see Fig. 6D). In contrast, high TBP:TP_{spring} loading ratios favored solitary greens; indeed, these taxa were more common late in the season after 2005 (Fig. 6E).

Finally, PCoA Axis 2 increased with water temperature (R^2 = 0.049; Fig. 8A, Table 3), indicating that cold temperatures favored cryptophytes and green algae while warm temperatures favored diatoms. Similar to the PCoA Axis 1 model, there appeared to be a thermal-threshold ~20°C which was not well-characterized by the model. Excluding a few cases, high values of PCoA Axis 2 were only observed at water temperatures greater than ~20°C.

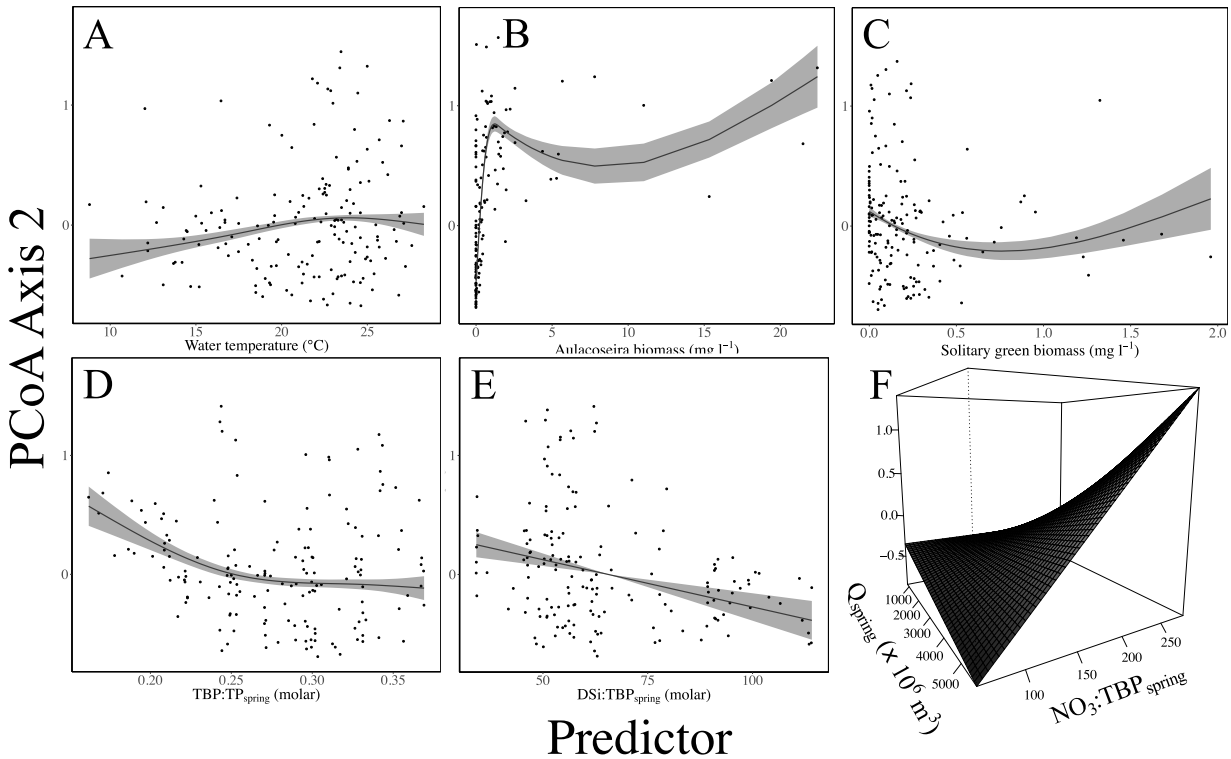

Figure 8. Panels A-E show estimated smoothing curves for 5 predictors of PCoA Axis 2. Positive values indicate higher relative diatom biomass while negative values indicate higher cryptophyte and chlorophytes relative biomass. The predictors are on the *x*-axis, and the curves show the contribution of the smoother to the fitted values. Bands and points, and axis label subscripts are as above. In F, the response surface is the smoother for the $Q_{spring} \times NO_3{:}TBP_{spring}$ interaction.

Spatial Patterns manuscript

Spatial-temporal modeling of phytoplankton dynamics

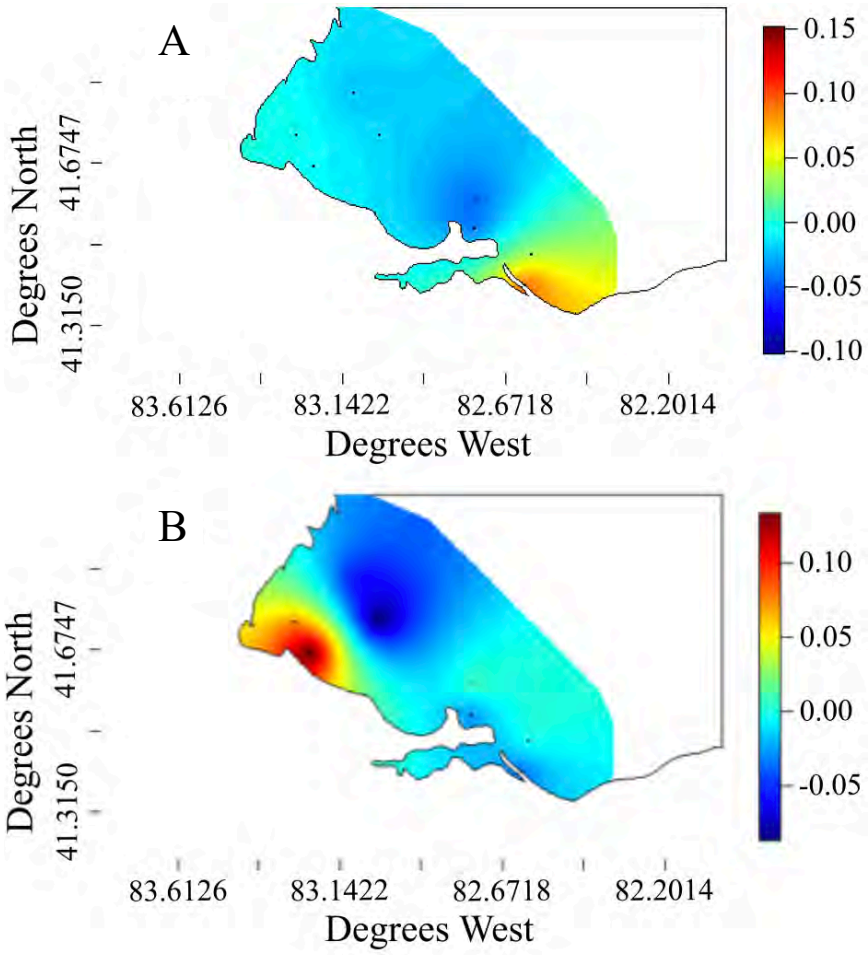

Figure 9. Spatial GAM model predictions of Western Basin of Lake Erie cyanobacterial biomass (log-transformed) in (A) pre-bloom years (1995-2002) and (B) bloom years (2003-2015). Data are averages over each time period. Black dots show the eight sampling locations in the Western Basin. Note the differences in the color scales.

These models are currently under development, but some preliminary results are shown in Figure 9. Briefly, cyanobacterial biomass was lower pre-2003, with the bulk of the biomass in the Western Basin concentrated to the southeast. When large-scale summer blooms began as a result of extreme, episodic eutrophication and warming, cyanobacterial biomass increased dramatically in the vicinity of the Maumee River mouth.

Discussion

The phytoplankton community in the WBLE has undergone a major compositional shift over the past two decades. While summer cyanobacterial blooms have become the norm (Bridgeman et al. 2012; Michalak et al. 2013; Stumpf et al. 2016), other phytoplankton taxa have also increased dramatically in abundance during the summer months. Maximum summer biomasses of diatoms, green algae and cryptophytes rose approximately five-fold between 1995 and 2015, primarily between 1995 and 2000. It is intriguing that these groups increased in biomass prior to what is considered the period of re-eutrophication. Overall, patterns in the composition of non-cyanobacterial phytoplankton indicate that recent increases in cyanobacteria blooms appear not to have had a negative effect on other phytoplankton, at the major groups level, many of which are relatively more edible to planktonic herbivores.

In addition to changes in composition and maximum abundance, our results also reveal changes in the phenology of cyanobacteria and diatoms. These groups exhibited distinct unimodal seasonal trends that changed from 1995 to 2015. As observed in other systems in conjunction with increasing water temperatures (Winder and Schindler 2004, Peeters et al. 2007), WBLE cyanobacteria blooms started earlier and ended later in 2015 relative 1995. The timing of peak cyanobacteria biomass changed from around 29 June in 1995 to 10 August in 2015 – a 40-day shift. These changes likely reflect a combination of warmer water temperatures and increased nutrient loading (see discussion below). The phenology of diatoms also changed from 1995 to 2015, exhibiting an earlier start and later end to the diatom bloom. Similar to the cyanobacteria, the date of peak diatom biomass changed from 10 July to 10 August – a 30-day shift. This shift in diatom phenology likely reflects the “blooms” (note: peak diatom biomass was always considerably lower than peak cyanobacteria biomass) of *Aulacoseira* sp. observed during the last decade of the LEPAS time series which our models associate with high NO_3:TBP loading ratios integrated between March and July.

Our model indicated that cyanobacteria biomass was highest at warm temperatures and following periods of both long- and short-term P loading. Cyanobacteria biomass (i.e., PCoA Axis 1) increased with water temperature up to the maximum temperature observed (28.3°C) and there appeared to be a threshold around 20°C above which the highest cyanobacteria biomasses were observed. Cyanobacteria biomass also increased with Q_{spring}, $Q_{14\text{-}day}$, and $TBP{:}TP_{spring}$ (when > 0.2); whereas, it declined with $DSi{:}TBP_{spring}$ and $NO_3{:}TBP_{14\text{-}day}$. Here, discharge (Q), which was also integrated over the given time period, should be considered a

general indicator of nutrient loading rate due to the high covariance among water, nutrient, sediment loads. Overall, metrics associated with long-term TBP loading explained two times as much variation in PCoA Axis 1 than those associated with short-term loading (43% versus 21%). Unfortunately, it is difficult to parse the relative contribution of the other nutrients involved in these ratios. Utilizing nutrient ratios in these models –with Q as a metric of total loading– was the only way to circumvent the high covariance among these predictor variables. Since it is unlikely that dissolved silica plays an important role in fueling cyanobacteria blooms, our working hypothesis is that TBP is driving these relationships

Our analysis of the drivers of cyanobacteria blooms in WBLE supports previous research with *Microcystis* spp. and other cyanobacteria species. Two major environmental drivers, high temperature and excessive TBP, are likely the most important drivers of summer cyanobacterial blooms (Klemer and Konopka 1989, Paerl and Huisman 2008, Stumpf et al. 2016). This hypothesis is founded on both decades of evidence from field studies (Smith 1983), and on the physiology of cyanobacteria, which commonly have higher thermal optima for population growth than other phytoplankton taxa (Robarts and Zohary 1987, Nalley et al. 2018), and which generally have a high demand for P, relative to N (Smith 1983, Klausmeier et al. 2008). Similarly, studies of Lake Erie's recent cyanobacterial blooms have implicated both climate change and increasing riverine inputs of TBP due to intensifying land use practices (Stumpf et al. 2012, Michalak et al. 2013, Stumpf et al. 2016).

Analysis of PCoA Axis 2 indicated that the relative balance between diatoms (high values) and greens/cryptophytes (low values) was shaped by water temperature as well as the spring loading ratios of NO_3:TBP, TBP:TP, and DSi:TBP. Low levels of TBP and high levels of NO_3 favored diatoms while the inverse favored green algae and the cryptophyte *Chroomonas* sp. Surprisingly, given the high Si requirements of diatoms (Sommer and Stabel 1983, Tilman et al. 1986, Conley and Kilham 1989, Thamatrakoln and Hildebrand 2008), diatom growth was favored when spring (March-July) DSi:TBP loading ratios were relatively low (<70). Indeed, while summer DSi:TBP decreased between 1995 and 2015, summer diatom biomass increased. It is important to note that high values of PCoA Axis 2 were associated with a high biomass of the diatom *Aulacoseira* sp which co-occurred with *Microcystis* sp. during blooms. Our results suggest that it is unlikely that Si limits diatom growth at our sampling location during the summer months and that N-limitation may play a role in mediating diatom growth in WBLE (Billen and Garnier 2007). Some researchers have argued that N-limitation is unlikely to exist in freshwater systems (Schindler et al. 2008, Schindler et al. 2016), though there is considerable

disagreement on this point (Elser et al. 2009a, Elser et al. 2009b, Paerl et al. 2016, O'Donnell et al. 2017). It is interesting to note that the short-term loading covariates did not play a role in the most likely model for PCoA Axis 2.

Our work supports previous research suggesting that cyanobacteria blooms are favored by warm temperatures (Paerl and Huisman 2008) and that climate warming will, therefore, promote larger cyanobacteria blooms. While there is little evidence that water temperatures in WBLE have been increasing (Mason et al. 2016, Zhong et al. 2018), a biologically important change in the timing of the peak summer temperature may have occurred, although this should be evaluated with a higher-frequency temperature dataset. The observed peak summer water temperature at our sampling location advanced by ~5 weeks earlier between 1995 and 2015. Concurrent with this shift, the summer maxima of cyanobacterial and diatom biomasses advanced by at least as much. We did not observe an interaction between water temperature and nutrient loading rates or ratios in either the PCoA Axis 1 or 2 models, suggesting that the effect of nutrients and temperature on phytoplankton biomass accumulation were additive and not synergistic (i.e., interactive) as suggested by Paerl and Huisman (2008).

In summary, between 1995 and 2015 there has been a distinct shift in phytoplankton total biomass and community structure in WBLE, which has been well documented. Our analyses make clear that interactions between water temperature and nutrient loading have greatly enhanced both cyanobacteria and diatom growth. We also show that green algae and cryptophytes exhibited higher biomass during this period of re-eutrophication. Our results to date (which focus primarily on the site nearest to the Maumee River mouth) indicate that temperature and TBP play an important role in shaping cyanobacteria biomass. In contrast, diatoms biomass increased with high rates of NO_3 loading and warm temperatures; whereas, green algae and the cryptophyte *Chroomonas* sp. were favored by cold water temperatures and high rates of TBP loading. Interestingly, cyanobacteria appeared to respond to variation in both short- and long-term loading; whereas, diatoms, greens, and *Chroomonas* sp. responded only to long-term loading. We also observed a considerable advance (> 30 days) in the phenology of both cyanobacteria and diatoms between 1995 and 2015, with an earlier onset and later end to the period of cyanobacteria dominance. Echoing Paerl and Huisman (2008), our results highlight that climate warming in conjunction with unchecked nutrient loading will only further increase both the size and duration of cyanobacteria blooms. While nutrient loading and cyanobacteria dominance did not have the impact on diatoms, greens, and cryptophytes that we expected our results indicated that warming might lead to a decline in both greens and

cryptophytes which could limit the quantity of edible algae available to zooplankton and higher trophic levels.

Acknowledgements

This project was funded through the Lake Erie Protection Fund (LEPF). The LEPF is supported by tax-deductible donation and voluntary contributions of Ohioans who purchase a Lake Erie license plate featuring the Marblehead lighthouse, Toledo Harbor lighthouse, or the Lake Erie life preserver. For more information, see www.lakeerie.ohio.gov. We thank Dr. L. Johnson and the Heidelberg National Center for Water Quality Research (NCWQR) for providing nutrient loading data as well as the United States Geological Survey (USGS) for providing discharge data for the Maumee River. Plankton analyses for the Lake Erie Plankton Abundance Survey (LEPAS) were funded by the Federal Aid in Sport Fish Restoration Program (F-69-P, Fish Management in Ohio, FADX09 to JMH, S. Ludsin, and formally Dr. D. Culver) administered jointly by the U.S. Fish and Wildlife Service and the Ohio Division of Wildlife. Dr. O'Donnell was supported by the Federal Aid in Sport Fish Restoration Program (FADX09 to JMH and S. Ludsin). We thank Dr. T. Royer and L. Sethna for analyses and intellectual contributions to early versions of this research. We also would like to thank technicians with the LEPAS program and at the Aquatic Ecology Laboratory (AEL) who have enumerated plankton samples for the LEPAS program. We are especially grateful to C. Doyle and M. Kulasa for their considerable contributions to the LEPAS program and to Dr. J. Stone for developing the LEPAS database. Finally, we would like to thank Dr. D. Culver for his decades of hard work and dedication to the development of the LEPAS program.

References

Baker, D. B., R. Confesor, D. E. Ewing, L. T. Johnson, J. W. Kramer, and B. J. Merryfield. 2014a. Phosphorus loading to Lake Erie from the Maumee, Sandusky and Cuyahoga rivers: The importance of bioavailability. Journal of Great Lakes Research **40**:502-517.

Baker, D. B., D. E. Ewing, L. T. Johnson, J. W. Kramer, B. J. Merryfield, R. B. Confesor, R. Peter Richards, and A. A. Roerdink. 2014b. Lagrangian analysis of the transport and processing of agricultural runoff in the lower Maumee River and Maumee Bay. Journal of Great Lakes Research **40**:479-495.

Billen, G., and J. Garnier. 2007. River basin nutrient delivery to the coastal sea: Assessing its potential to sustain new production of non-siliceous algae. Marine Chemistry **106**:148-160.

Boegman, L., M. R. Loewen, D. A. Culver, P. F. Hamblin, and M. N. Charlton. 2008. Spatial-Dynamic Modeling of Algal Biomass in Lake Erie: Relative Impacts of Dreissenid Mussels and Nutrient Loads. Journal of Environmental Engineering **134**:456-468.

Bridgeman, T. B., J. D. Chaffin, D. D. Kane, J. D. Conroy, S. E. Panek, and P. M. Armenio. 2012. From River to Lake: Phosphorus partitioning and algal community compositional changes in Western Lake Erie. Journal of Great Lakes Research **38**:90-97.

Briland, R. 2018. Evaluating the causes and consequences of ecosystem change in Lake Erie: From plankton to fish. The Ohio State University, Columbus, OH USA.

Brooks, B. W., J. M. Lazorchak, M. D. Howard, M. V. Johnson, S. L. Morton, D. A. Perkins, E. D. Reavie, G. I. Scott, S. A. Smith, and J. A. Steevens. 2016. Are harmful algal blooms becoming the greatest inland water quality threat to public health and aquatic ecosystems? Environ Toxicol Chem **35**:6-13.

Carey, C. C., B. L. Brown, and K. L. Cottingham. 2017. The cyanobacterium *Gloeotrichia echinulata* increases the stability and network complexity of phytoplankton communities. Ecosphere **8**:1-14.

Chaffin, J. D., T. B. Bridgeman, S. A. Heckathorn, and S. Mishra. 2011. Assessment of Microcystis growth rate potential and nutrient status across a trophic gradient in western Lake Erie. Journal of Great Lakes Research **37**:92-100.

Conley, D. J., and S. S. Kilham. 1989. Differences in silica content between marine and freshwater diatoms. Limnology and Oceanography **34**:205-213.

Cox, S. L., M. J. Witt, C. B. Embling, B. J. Godley, P. J. Hosegood, P. I. Miller, S. C. Votier, and S. N. Ingram. 2017. Temporal patterns in habitat use by small cetaceans at an oceanographically dynamic marine renewable energy test site in the Celtic Sea. Deep Sea Research Part II: Topical Studies in Oceanography **141**:178-190.

Elser, J., M. Kyle, L. Steger, K. R. Nydick, and J. S. Baron. 2009a. Nutrient availability and phytoplankton nutrient limitation across a gradient of atmospheric nitrogen deposition. Ecology **90**:3062-3073.

Elser, J. J., T. Andersen, J. S. Baron, A. Bergstrom, M. Jansson, M. Kyle, K. R. Nydick, L. Steger, and D. O. Hessen. 2009b. Shifts in lake N:P stoichiometry and nutrient limitation driven by atmospheric nitrogen deposition. Science **326**.

Hampton, S. E., E. E. Holmes, L. P. Scheef, M. D. Scheuerell, S. L. Katz, D. E. Pendleton, and E. J. Ward. 2013. Quantifying effects of abiotic and biotic drivers on community dynamics with multivariate autoregressive (MAR) models. Ecology **94**:2663-2669.

Hampton, S. E., L. R. Izmest'Eva, M. V. Moore, S. L. Katz, B. Dennis, and E. A. Silow. 2008. Sixty years of environmental change in the world's largest freshwater lake - Lake Baikal, Siberia. Global Change Biology **14**:1947-1958.

Hampton, S. E., M. D. Scheuerell, and D. E. Schindler. 2006. Coalescence in the Lake Washington story: Interaction strengths in a planktonic food web. Limnology and Oceanography **51**:2042-2051.

Ho, J. C., and A. M. Michalak. 2017. Phytoplankton blooms in Lake Erie impacted by both long-term and springtime phosphorus loading. Journal of Great Lakes Research **43**:221-228.

Holmes, E., E. J. Ward, M. Scheuerell, and K. Wills. 2012. MARSS: multivariate autoregressive state-space models for analyzing time-series data. The R Journal **4**:11-19.

Holmes, E., E. J. Ward, M. Scheuerell, and K. Wills. 2018. MARSS: multivariate autoregressive state-space modeling. NOAA, Seattle, USA.

Ives, A. R., B. Dennis, K. L. Cottingham, and S. R. Carpenter. 2003. Estimating community stability and ecological interactions from time-series data. Ecological Monographs **73**:301-330.

Kane, D. D., J. D. Conroy, R. Peter Richards, D. B. Baker, and D. A. Culver. 2014. Re-eutrophication of Lake Erie: Correlations between tributary nutrient loads and phytoplankton biomass. Journal of Great Lakes Research **40**:496-501.

Kane, D. D., S. I. Gordon, M. Munawar, M. N. Charlton, and D. A. Culver. 2009. The Planktonic Index of Biotic Integrity (P-IBI): An approach for assessing lake ecosystem health. Ecological Indicators **9**:1234-1247.

Klausmeier, C. A., E. Litchman, T. Daufresne, and S. A. Levin. 2008. Phytoplankton stoichiometry. Ecological Research **23**:479-485.

Klemer, A. R., and A. E. Konopka. 1989. Causes and Consequences of Blue-Green Algal (Cyanobacterial) Blooms. Lake and Reservoir Management **5**:9-19.

Lindgren, F., H. Rue, and J. Lindstrom. 2011. An explicit link between Gaussian fields and Gaussian Markov random fields: the SPDE approach (with discussion). Journal of the Royal Statistical Society, Series B **73**:423-498.

Mason, L. A., C. M. Riseng, A. D. Gronewold, E. S. Rutherford, J. Wang, A. Clites, S. D. P. Smith, and P. B. McIntyre. 2016. Fine-scale spatial variation in ice cover and surface temperature trends across the surface of the Laurentian Great Lakes. Climatic Change **138**:71-83.

Michalak, A. M., E. J. Anderson, D. Beletsky, S. Boland, N. S. Bosch, T. B. Bridgeman, J. D. Chaffin, K. Cho, R. Confesor, I. Daloglu, J. V. Depinto, M. A. Evans, G. L. Fahnenstiel, L. He, J. C. Ho, L. Jenkins, T. H. Johengen, K. C. Kuo, E. Laporte, X. Liu, M. R. McWilliams, M. R. Moore, D. J. Posselt, R. P. Richards, D. Scavia, A. L. Steiner, E. Verhamme, D. M. Wright, and M. A. Zagorski. 2013. Record-setting algal bloom in Lake Erie caused by agricultural and meteorological trends consistent with expected future conditions. Proc Natl Acad Sci U S A **110**:6448-6452.

Nalley, J. O., D. R. O'Donnell, and E. Litchman. 2018. Temperature effects on growth rates and fatty acid content in freshwater algae and cyanobacteria. Algal Research **35**:500-507.

O’Donnell, D. R., P. Wilburn, E. A. Silow, L. Y. Yampolsky, and E. Litchman. 2017. Nitrogen and phosphorus colimitation of phytoplankton in Lake Baikal: Insights from a spatial survey and nutrient enrichment experiments. Limnology and Oceanography **62**:1383-1392.

Oksanen, J., F. G. Blanchet, M. Friendly, R. Kindt, P. Legendre, D. McGlinn, P. R. Minchin, R. B. O’Hara, G. L. Simpson, P. Solymos, M. H. H. Stevens, E. Szoecs, and H. Wagner. 2018. vegan: Community Ecology Package.

Paerl, H. W., N. S. Hall, and E. S. Calandrino. 2011. Controlling harmful cyanobacteria blooms in a world experiencing anthropogenic and climatic -induced change. Science of the Total Environment **409**:1739-1745.

Paerl, H. W., and J. Huisman. 2008. Blooms like it hot. Science **320**:57-58.

Paerl, H. W., J. T. Scott, M. J. McCarthy, S. E. Newell, W. S. Gardner, K. E. Havens, D. K. Hoffman, S. W. Wilhelm, and W. A. Wurtsbaugh. 2016. It Takes Two to Tango: When and Where Dual Nutrient (N & P) Reductions Are Needed to Protect Lakes and Downstream Ecosystems. Environ Sci Technol **50**:10805-10813.

Peeters, F., D. Straile, A. Lorke, and D. M. Livingstone. 2007. Earlier onset of the spring phytoplankton bloom in lakes of the temperate zone in a warmer climate. Global Change Biology **13**:1898-1909.

Robarts, R. D., and T. Zohary. 1987. Temperature effects on photosynthetic capacity, respiration, and growth rates of bloom-forming cyanobacteria. New Zealand Journal of Marine and Freshwater Research **21**:391-399.

Roy, E. D., J. F. Martin, E. G. Irwin, J. D. Conroy, and D. A. Culver. 2010. Transient social-ecological stability: the effects of invasive species and ecosystem restoration on nutrient management compromise in Lake Erie. Ecology and Society **15**:20.

Rue, H., H. Martino, and N. Chopin. 2009. Approximate BAyesian inference for latent Gaussian models using integrated nested Laplace approximations (with discussion). Journal of the Royal Statistical Society, Series B **71**:319-392.

Scavia, D., J. David Allan, K. K. Arend, S. Bartell, D. Beletsky, N. S. Bosch, S. B. Brandt, R. D. Briland, I. Daloğlu, J. V. DePinto, D. M. Dolan, M. A. Evans, T. M. Farmer, D. Goto, H. Han, T. O. Höök, R. Knight, S. A. Ludsin, D. Mason, A. M. Michalak, R. Peter Richards, J. J. Roberts, D. K. Rucinski, E. Rutherford, D. J. Schwab, T. M. Sesterhenn, H. Zhang, and Y. Zhou. 2014. Assessing and addressing the re-eutrophication of Lake Erie: Central basin hypoxia. Journal of Great Lakes Research **40**:226-246.

Schindler, D. W., S. R. Carpenter, S. C. Chapra, R. E. Hecky, and D. M. Orihel. 2016. Reducing Phosphorus to Curb Lake Eutrophication is a Success. Environ Sci Technol **50**:8923-8929.

Schindler, D. W., R. E. Hecky, D. L. Findlay, M. P. Stainton, B. R. Parker, M. J. Paterson, K. G. Beaty, M. Lyng, and S. E. M. Kasian. 2008. Eutrophication of lakes cannot be controlled by reducing nitrogen input: Results of a 37-year whole-ecolosystem experiment. Proceedings of the National Acadamy of Science **105**:11254-11258.

Smith, V. H. 1983. Low nitrogen to phosphorus ratios favor dominance by blue-green algae in lake phytoplankton. Science **221**:669-671.

Sommer, U., R. Adrian, L. De Senerpont Domis, J. J. Elser, U. Gaedke, B. Ibelings, E. Jeppesen, M. Lürling, J. C. Molinero, W. M. Mooij, E. van Donk, and M. Winder. 2012.

Beyond the Plankton Ecology Group (PEG) Model: Mechanisms Driving Plankton Succession. Annual Review of Ecology, Evolution, and Systematics **43**:429-448.

Sommer, U., Z. M. Gliwicz, W. Lampert, and A. Duncan. 1986. The PEG-model of seasonal succession of planktonic events in fresh waters. Arch. Hydrobiol. **106**:433-471.

Sommer, U., and H. H. Stabel. 1983. Silicon consumption and population density changes of dominant planktonic diatoms in Lake Constance. Journal of Ecology **71**:119-130.

Stow, C. A., Y. Cha, L. T. Johnson, R. Confesor, and R. P. Richards. 2015. Long-term and seasonal trend decomposition of Maumee River nutrient inputs to western Lake Erie. Environ Sci Technol **49**:3392-3400.

Stumpf, R. P., L. T. Johnson, T. T. Wynne, and D. B. Baker. 2016. Forecasting annual cyanobacterial bloom biomass to inform management decisions in Lake Erie. Journal of Great Lakes Research **42**:1174-1183.

Stumpf, R. P., T. T. Wynne, D. B. Baker, and G. L. Fahnenstiel. 2012. Interannual variability of cyanobacterial blooms in Lake Erie. Plos One **7**:e42444.

Thamatrakoln, K., and M. Hildebrand. 2008. Silicon uptake in diatoms revisited: a model for saturable and nonsaturable uptake kinetics and the role of silicon transporters. Plant Physiol **146**:1397-1407.

Tilman, D., R. Kiesling, R. Sterner, S. S. Kilham, and F. A. Johnson. 1986. Green, bluegreen, and diatom algae: Taxonomic differences in competitive ability for phosphorus, silicon, and nitrogen. Arch. Hydrobiol. **106**:473-485.

Watson, S. B., C. Miller, G. Arhonditsis, G. L. Boyer, W. Carmichael, M. N. Charlton, R. Confesor, D. C. Depew, T. O. Höök, S. A. Ludsin, G. Matisoff, S. P. McElmurry, M. W. Murray, R. Peter Richards, Y. R. Rao, M. M. Steffen, and S. W. Wilhelm. 2016. The re-eutrophication of Lake Erie: Harmful algal blooms and hypoxia. Harmful Algae **56**:44-66.

Winder, M., and D. E. Schindler. 2004. Climatic effects on the phenology of lake processes. Global Change Biology **10**:1844-1856.

Wood, S. N. 2006. Generalized additive models: an introduction with R. Taylor & Francis, Boca Raton, FL USA.

Wood, S. N. 2019. mgcv: mixed GAM computation vehicle with automatic smoothness estimation. R Core Team 2017.

Yuan, F., R. Depew, and C. Soltis-Muth. 2014. Ecosystem regime change inferred from the distribution of trace metals in Lake Erie sediments. Sci Rep **4**:7265.

Zhang, H., L. Boegman, D. Scavia, and D. A. Culver. 2016. Spatial distributions of external and internal phosphorus loads in Lake Erie and their impacts on phytoplankton and water quality. Journal of Great Lakes Research **42**:1212-1227.

Zhang, H., D. A. Culver, and L. Boegman. 2008. A two-dimensional ecological model of Lake Erie: Application to estimate dreissenid impacts on large lake plankton populations. Ecological Modelling **214**:219-241.

Zhong, Y., M. Notaro, and S. J. Vavrus. 2018. Spatially variable warming of the Laurentian Great Lakes: an interaction of bathymetry and climate. Climate Dynamics **52**:5833-5848.

Zuur, A. F., and E. N. Ieno. 2018. Beginner's guide to spatial, temporal, and spatial-temporal ecological data analysis with R-INLA Volume II: GAM and zero-inflated models. Highland Statistics, Newburgh, UK.

Zuur, A. F., E. N. Ieno, and A. A. Saveliev. 2017. Beginner's guide to spatial, temporal, and spatial-temporal ecological data analysis with R-INLA Volume I: Using GLM and GLMM. Highland Statistics, Newburgh, UK.

Zuur, A. F., E. N. Ieno, N. Walker, A. A. Saveliev, and G. M. Smith. 2009. Mixed models and extensions in ecology with R. Springer, New York, USA.